Tikrit Journal of Engineering Sciences

IRAQI Academic Scientific Journals | TJES Tikrit Journal of Engineering Sciences

Article | Tikrit Journal of Engineering Sciences (2026); 33(3): 3136

Open Access

Integrated Experimental and Modeling Study of Organic Pollutants Adsorption from Real Municipal Wastewater Using Anthracite-Based Activated Carbon

Noor A. Awad [1], Maha A. Dawood [1], Sanarya K. Kamal [2], Ammar S. Abbas [3*], Ali A. Taresh [4], Seyed Reza Shabanian[4], Vida Ravankhah [5]

[1] Fuel and Energy Engineering Department, Oil and Gas Techniques Engineering College, Northern Technical University, Kirkuk, Iraq.
[2] Laboratories and Quality Control Department, Water Division, North Gas Company, Ministry of Oil, Kirkuk, Iraq.
[3] Chemical Engineering Department, College of Engineering, Baghdad University, Baghdad, Iraq.
[4] Department of Chemical Engineering, Babol Noshirvani University of Technology, Babol, Iran.
[5] Chemical Engineering Department, Faculty of Engineering, Kermanshah University of Technology, Kermanshah, Iran.

Emails:
Noor A. Awad | Maha A. Dawood | Sanarya K. Kamal | Ammar S. Abbas | Ali A. Taresh | Seyed Reza Shabanian | Vida Ravankhah

Abstract:

This study presents experimental and simulation results for the adsorption of organic pollutants from real municipal wastewater using anthracite-based activated carbon adsorption. This work combines experimental design to investigate adsorption isotherms and kinetics with mathematical modeling to support process analysis and performance prediction for a fixed-bed adsorption column. The results showed that a Sips-type adsorption isotherm model was the most suitable for describing the adsorption curve (R^2= 0.9782), with a saturation value of 156.38 mg/g, and the kinetic data of the adsorption of organic pollutants followed a second-order kinetic model (R^2= 0.8998). Based on the experimental results, a transfer-dispersion-adsorption model was developed for a fixed-bed adsorption column to simulate the breakthrough curve and evaluate the dynamic performance of the adsorption process. The proposed model was used to predict column efficiency and service life, and to evaluate the impact of key design and operational variables (interfacial flow velocity, adsorbent bed height, and inlet pollutant concentration), providing valuable insights for process design and scaling. The integrated experimental modeling framework demonstrated the feasibility of selecting a fixed-bed adsorber for efficient treatment of real municipal wastewater. The current adsorbent emerged as a promising adsorbent for this type of treatment and performed successfully in simulation scenarios of fixed-bed adsorption units for various wastewater treatment applications.

Keywords:

Anthracite-based activated carbon adsorption; Breakthrough curve prediction; Fixed-bed adsorption column; Municipal wastewater treatment; Organic matter removal; Process modeling and simulation.

Highlights:

- Adsorbent was used to reduce the organic load on municipal wastewater.
- Adsorption was analyzed using equilibrium, kinetic, and diffusion models.
- Batch-derived parameters were used to build a fixed-bed column model.
- Effects of flow rate, particle size, influent concentration, and bed height were assessed.
- Breakthrough curves quantified the performance of fixed-bed adsorption.

Corresponding Author*:

Ammar S. Abbas
Chemical Engineering Department, College of Engineering, Baghdad University, Baghdad, Iraq.

Article History:

Received:	01	Apr.	2026
Received in revised form:	20	Apr.	2026
Accepted:	18	May	2026
Final Proofreading:	28	Sep.	2026
Available online:	15	Oct.	2026

Citation:

Awad NA, Dawood MA, Kamal SK, Abbas AS, Taresh AA, Shabanian SR, Ravankhah V. **Integrated Experimental and Modeling Study of Organic Pollutants Adsorption from Real Municipal Wastewater Using Anthracite-Based Activated Carbon**. *Tikrit Journal of Engineering Sciences* 2026; **33**(3): 3136.

https://doi.org/10.25130/tjes.33.3.2

© This Is an Open Access Article Under the cc by License. http://creativecommons.org/licenses/by/4.0/

1.INTRODUCTION

Water is one of the most important resources for all known life forms and is essential to supporting global development sectors. This includes its use in multiple fields, including domestic use, agriculture, industry, and energy production, which produce large quantities of polluted water, thus making access to clean water a key factor in achieving the United Nations Sustainable Development Goals [1]. Providing clean water is vital for achieving sustainable development and protecting human health and the environment. Thus, with the passage of time and population growth, the need to treat polluted wastewater has increased to provide clean water suitable for reuse and to reduce the negative effects of pollutants on various ecosystems [2]. Municipal wastewater contains a complex mixture of organic pollutants that pose serious health challenges and environmental risks. Municipal wastewater typically contains various hydrocarbons [3], phenolic compounds [4], pharmaceuticals and personal care products [5], endocrine-disrupting chemicals [6], pesticides, and microplastics that act as vectors for other toxins [7]. Wastewater can be considered severely polluted if the values of both the chemical and biological oxygen demand (COD and BOD) rise to several hundred or even thousands of milligrams per liter (mg/L) [8]. Strict international regulations regarding wastewater are now being implemented worldwide, due to the environmental and health risks posed by organic pollutants [9]. With the aim of promoting public human health protection, the World Health Organization (WHO) recommends limits of between 100 and 125 mg/L for COD and more conservative levels for BOD, ranging between 20 and 30 mg/L, and limits for total suspended solids (TSS) of 30 mg/L, for wastewater from industrial and agricultural activities [10]. In Iraq, regulations governing surface water waste disposal have stricter requirements than those set by the WHO for COD. Local Iraqi regulations stipulate a COD of 100 mg/L or less; however, they have a slightly broader BOD range (up to 40 mg/L), and no more than 60 mg/L of TSS for industrial wastewater to be discharged to the surface waters. Nowadays, compliance with local standards and the development of wastewater treatment units are essential to eliminate pollutants and the environmental burden they cause; they have become a vital element in the sustainable water economy, facilitating the reuse of water in agriculture and industry, and even indirectly for the reuse of drinking water in some areas [11]. Wastewater treatment technologies are generally classified into biological, chemical, and physical processes [12]. Biological wastewater treatment processes rely primarily on microbial metabolism, where microorganisms convert biodegradable organic pollutants into simpler, less harmful end products [13]. However, these processes are limited in terms of treatment speed and can be affected by the concentrations of certain pollutants, which may be present at levels lethal to microorganisms [14]. Chemical treatment methods involve the direct or indirect use of chemicals to promote pollutant removal, but they can also produce secondary pollutants, such as chemical sludge, and potentially hazardous byproducts [15,16]. Physical treatment techniques rely on the principles of physics to separate pollutants from wastewater, such as sedimentation, filtration, flotation, membrane separation, and adsorption techniques [17]. The adsorption process relies on trapping pollutants on the surface of adsorbent solids using van der Waals forces, chemical reactions, or a combination of both. Adsorption technology has proven highly efficient in removing various organic pollutants such as dyes, pharmaceuticals, phenolic compounds, and pesticides [18,19]. Several potential adsorbents for specific pollutant removal have been investigated, such as zeolites [20,21], starch-based polymers [22,23], bio-composites [24], and various types of activated carbon (AC) [25–27]. AC remains the most well-known and widely used adsorbent for removing organic pollutants and dyes [28,29]. Various types of AC have been prepared from different sources, industrial byproducts, and agricultural waste [30–32]. In this context, anthracite has emerged as a practical and less expensive alternative with good mechanical and surface properties. Experimental evidence has shown that raw anthracite is able to effectively remove organic matter from domestic wastewater under continuous flow conditions [33], with stable performance in fixed-bed systems due to its structural durability [34]. Anthracite-based activated carbon (ABAC) has emerged as a promising and low-cost adsorbent due to its high porosity, large surface area, and mechanical stability [33,35]. Materials suitable for use in continuous, fixed-bed adsorbents are attractive areas for research and development [36]. This process-focused study aims to evaluate the performance of ABAC as a potential adsorbent for treating municipal wastewater collected from a wastewater treatment plant serving a residential area. The study includes a preliminary characterization of the commercially available suggested adsorbent (ABAC) in terms of its surface area and pore volume. The study also involves a comprehensive experimental investigation to understand the adsorption behavior of ABAC for COD under typical operating conditions, by determining the equilibrium adsorption isotherms and adsorption kinetics. Following this, a mathematical model will be developed,

utilizing the laboratory results, to simulate a proposed fixed-bed continuous adsorption column. The proposed modeling framework will be used to predict the influence of wastewater interfacial velocity, column bed height, and inlet pollutant concentrations on the behavior of the breakthrough curves, column efficiency, and adsorption operating time. The simulation results will provide analytical support for process and design considerations and will evaluate the expected performance of adsorption columns used in real-world municipal wastewater treatment applications.

2.EXPERIMENTAL WORK

The adsorption performance of ABAC to reduce organic load (measured as COD, mg/L) was studied from real municipal wastewater samples collected from a municipal wastewater treatment unit serving a residential area in Kirkuk, Iraq. The ABAC was washed with deionized water until the washing water remained clear, removing any impurities and fine particles. The washed ABAC was then dried in a laboratory oven at 105°C for 2 hours to remove all moisture and stored in a desiccant until used. The ABAC of a particle size range of 0.06–1.2 mm was selected for the adsorption-based COD removal from wastewater. The essential properties of the adsorbent, such as surface area and pore size, were also determined using N_2 adsorption/absorption analysis using the Micromeritics ASAP 2020 device located at the Petroleum Research and Development Center of the Ministry of Oil (Iraq). Batch experiments to study adsorption equilibrium using adsorption isotherms were conducted by contacting various ABAC doses (0.25 to 2.00 g/L) with a constant COD concentration (156 mg/L) in municipal wastewater under constant agitation via a shaker (150 rpm) at ambient conditions until equilibrium was reached after 24 h. The COD amount adsorbed per weight of ABAC adsorbent at equilibrium (q_e) was calculated using Eq. (1).

$$q_e = (C_o - C_e) \times \frac{V}{m} \quad \textbf{(1)}$$

Where q_e represents the equilibrium concentration of adsorbate in the adsorbent phase (mg adsorbate/g adsorbent), C_o is the initial concentration of ABAC in the fluid phase (mg/L), C_e is the equilibrium concentration of adsorbate in the liquid phase (mg/L), V is the volume of fluid phase (L), and m is the mass of the adsorbent (g).

The adsorption kinetics were also studied by monitoring the COD concentration over time (C_t) for up to 2 h, using 1 gram of ABAC per liter of wastewater. For all samples examined, 5 ml of the sample was withdrawn and filtered, and the residual COD concentration was then measured using the closed-loop reflux colorimetry method with a DR6000 spectrometer. The resulting data were then analyzed using multiple isothermal and kinetic models to gain a deeper understanding of the adsorption process.

3.RESULTS AND DISCUSSION

The results of pore structure characteristics tests, obtained using nitrogen adsorption-desorption techniques, indicated that the surface area and pore volume of ABAC are 1264.28 m^2/g and 0.6422 cm^3/g, respectively. The high surface area and suitable pore volume strongly suggest the potential of this material as a promising adsorption medium for organic pollutants from real wastewater. The adsorption phenomenon at equilibrium was studied by developing a suitable isotherm equilibrium model to describe the relationship between the equilibrium concentration (C_e) of the organic load, as an indicator of the COD, and the amount of organic matter adsorbed onto the surface of the adsorbent. Figure 1 shows the experimental results for the equilibrium capacity (q_e), which is directly proportional to the C_e (black points), while the colored curves correspond to different adsorption isotherm models used to interpret the adsorption behavior. The experimental results showed that the adsorption capacity was low at an equilibrium concentration (51.5 mg/L), which was obtained using the highest amount of ABAC (2 g). This is attributed to the presence of an excess of adsorbent required for the adsorption of organic material. Conversely, the equilibrium concentration increases as the amount of adsorbent decreases, leading to an increase in the equilibrium adsorption capacity to its highest value (286.96 mg/g), which was recorded using the lowest tested amount of adsorbent (0.25 g per liter). These results showed good agreement with the previously reported [37]. This tendency suggests that the driving force for mass transfer becomes stronger as the concentration gradient between the solution and the adsorbent surface increases [38].

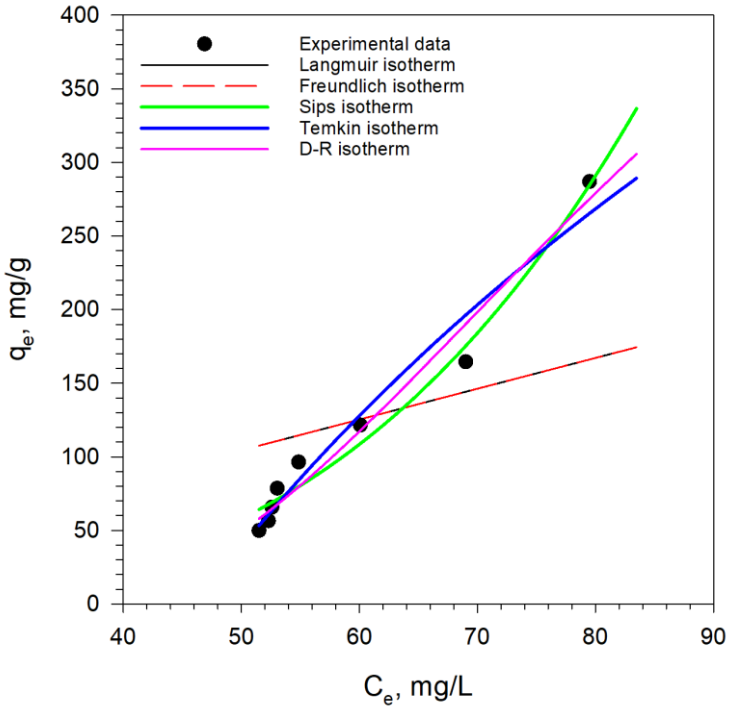


Fig. 1 Equilibrium COD Adsorption Capacity Versus the Initial Concentration After 24 h of Adsorption At 25 °C.

3.1.The Adsorption Isotherm Models

The two-parameter isotherms, which are widely recognized, were selected to characterize the adsorption of organic matter (as COD) on ABAC [39, 40]. The isotherm models employed include Langmuir, Freundlich, Temkin, Dubinin-Radushkevich (D–R), and Sips models. All calculated values of the models' parameters were listed later in Table 1.

3.1.1.Langmuir Adsorption Isotherm Model

The Langmuir adsorption isothermal model (LAIM) [41] is an empirical construct that posits that adsorption occurs exclusively at a finite number of specific sites, with no lateral interactions occurring among the adsorbed molecules. LAIM is represented by a non-linear equation as demonstrated in Eq. (2).

$$q_e = \frac{q_{\max} b C_e}{1 + b C_e} \qquad \textbf{(2)}$$

Where q_e denotes the quantity of adsorbate in the adsorbent at equilibrium (mg/g), q_{max} represents the maximum monolayer coverage capacity (mg/g), and b signifies the constant of LAIM or the energy or net enthalpy of adsorption (L/mg).

The LAIM proved inadequate for accurately analyzing the adsorption of COD onto ABAC. The computed coefficient of determination (R^2) was 0.4418 and a high root mean square error (RMSE) value (55.29 mg/g), indicating a poor fit to the experimental data, and that the model is inapplicable in elucidating the adsorption processes under the conditions investigated. Furthermore, the maximum adsorption capacity (374.73 mg/g) calculated was excessively high, further substantiating that the LAIM is not a suitable representation.

3.1.2.Freundlich Adsorption Isotherm Model

The non-ideal and reversible adsorption phenomena within multilayer heterogeneous adsorption contexts are quantitatively represented by Freundlich adsorption isotherm model (FAIM) [42] as in Eq. (3).

$$q_e = K_F C_e^{1/n} \qquad \textbf{(3)}$$

wherein K_F signifies the Freundlich constant indicative of the relative adsorption capacity (mg/g), and n denotes the heterogeneity factor that characterizes the adsorption intensity. The FAIM exhibited inadequate performance when aligned with the experimental data, yielding a relatively low correlation coefficient of 0.4419 as an R^2 value, and a high RMSE value (55.82 mg/g), as shown in Table 1.

3.1.3.Temkin Adsorption Isotherm Model

The Temkin adsorption isotherm model (TAIM) posits a linear relationship between the heat of adsorption of all molecules within the layer and the extent of coverage, stemming from the interactions between adsorbent and adsorbate. The model can be expressed as in Eq. (4) [43].

$$q_e = \frac{RT}{b_T} \ln k_T C_e \qquad \textbf{(4)}$$

k_T represents the equilibrium binding constant of the Temkin isotherm (L/g), universal gas constant (8.314 J/mol K), T represents temperature in K, and b_T: Temkin isotherm constant, while $B = RT/b_T$ denotes a constant that correlates with the heat of adsorption. The

TAIM exhibited a commendable fit to the experimental data, achieving an R^2 value of 0.9582 and a relatively low RMSE value (15.13 mg/g). The derived constants were B = 488.27 and k_T = 0.02166 L/g as shown in Table 1. The comparatively high R^2 value substantiates the existence of adsorbent-adsorbate interactions within the adsorption process.

3.1.4.Dubinin-Radushkevich (D-R) Adsorption Isotherm Model

The D-R adsorption isotherm model (DRAIM) is an empirical framework that articulates the dynamics of the adsorption process, which occurs following the establishment of a pore-filling mechanism [44], as shown in Eq. (5).

$$q_e = q_s e^{-K_{ad}\varepsilon^2} \quad \textbf{(5)}$$

q_s denotes the theoretical saturation capacity (mg/g), K_{ad} is the constant associated with the mean free energy of D–R isotherm constant adsorption (mol²/kJ²), and ε represents D–R isotherm constant. The DRAIM also provided an excellent fit to the experimental data, achieving an R^2 value of 0.9698 with RMSE equal to 12.86 mg/g. The determined saturation capacity (q_s) was 859.06 mg/g, and the K_{ad} constant was 1186.91 mol²/kJ². The apparent energy of adsorption (E) was calculated using Eq. (6).

$$E = \frac{1}{2K_{ad}} \quad \textbf{(6)}$$

where K_{ad} is the D-R constant (mol²/kJ²), the computed mean adsorption energy was 20.5J/mol. The low positive value of E, alongside the reported heat of physical adsorption in the liquid phase, is consistent with the existing literature [45].

3.1.5.Sips Adsorption Isotherm Equation

The Sips adsorption isotherm model (SAIM) constitutes a composite formulation that integrates elements of both LAIM and FAIM, as expressed in Eq. (7).

$$q_e = q_{\max} \frac{\left(K_s C_e\right)^{n_s}}{\left(1+\left(K_s C_e\right)^{n_s}\right)} \quad \textbf{(7)}$$

Where K_s represents the Sips model constant in L/mg, and n_s denotes the exponent of the SAIM. Among the investigated models, the Sips isotherm provided the best fit to the adsorption isotherm experimental data, as indicated by the highest correlation coefficient (R^2 = 0.9782) and the lowest RMSE value (10.94 mg/g), as shown in Table 1.

The maximum adsorption capacity (q_{max}) was determined to be 156.38 mg/g, with the Sips equilibrium constant (K_s) quantified at 0.001019, and the heterogeneity exponent (n_s) measured at 3.42.

Table 1 Constants for Each of the Equilibrium Isotherm Models and R^2.

Isotherm model	Model parameters	Parameter value	R^2, -	RMSE, mg/g
LAIM	q_m, (mg/g)	374.73	0.4418	55.29
	K_L, (l/mg)	5.58E-08		
FAIM	K_F, (mg^{1-n} l^n/g)	2.09	0.4419	55.82
	n, (-)	1.00		
TAIM	RT/b_T= B, J/mol	488.2725	0.9582	15.13
	ln k_T,k_T in l/g	0.02166		
DRAIM	q_D, (mg/g)	859.0602	0.9698	12.86
	K_{DR}, (mol²/kJ²)	1186.908		
	E, (J/mol)	20.525		
SAIM	q_s, (mg/g)	156.38	0.9782	10.94
	K_s, (l/mg)	0.001019		
	n_s, (-)	3.42		

3.2.Adsorption Kinetics

The kinetics pertaining to the adsorption of organic matter onto ABAC were examined by monitoring the concentration of the organic pollutants in the treated wastewater over time (C_t), and the organic removal was obtained, as illustrated in Fig. 2. The results indicate that removal efficiency increased sharply during the first 30 min (reached 45.7%), then gradually increased until it reached 60.1% after 120 min from the start of the adsorption process. No significant increase in the organic pollutants' removal was observed after two hours, up to 180 minutes, achieving a consistent removal efficiency of 63.5%, alongside a residual organic concentration in the treated wastewater of 54 mg/L (as COD). The fact that the removal and/or concentration values remained almost constant at the end of the kinetic equilibrium experiment confirms the claim that equilibrium was fully achieved. The two kinetic models utilized, the pseudo-first order (PFO) and pseudo-second order (PSO), were applied to the experimental data, as shown in Eqs. (8) and (9) were solved through linear regression employing the least-squares method to determine the adsorption rate constants (k_1, and k_2) for each model (46, 47).

$$\frac{dq}{dt} = k_1 \frac{q_e}{q}(q_e - q) \quad \textbf{(8)}$$

$$\frac{dq}{dt} = k_2 (q_e - q)^2 \quad \textbf{(9)}$$

where q_e and q_t signify the adsorption capacity of the organic matter at equilibrium (mg/g) and the adsorption capacity at any given time, both were in mg/g. k_1 as the PFO adsorption rate constant (1/min), and k_2 as the PSO adsorption rate constant (g/mg.min).

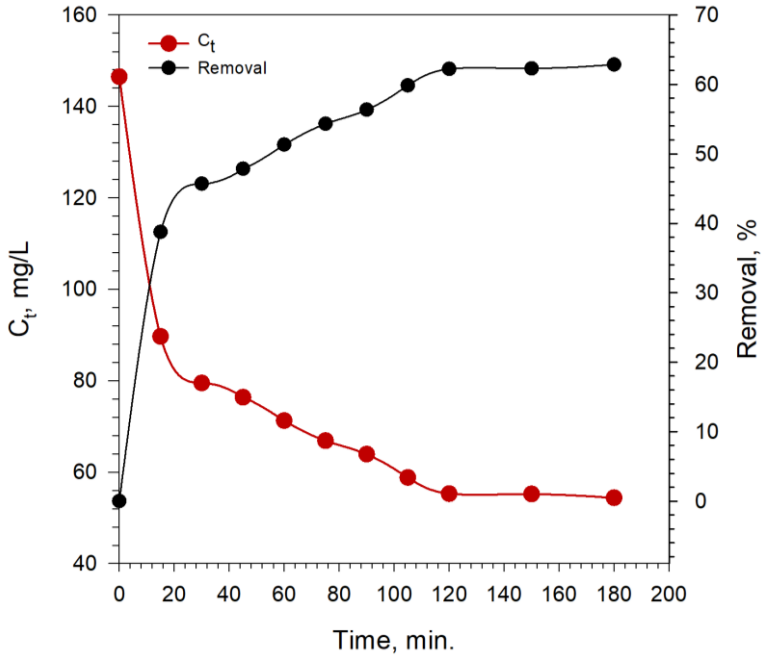


Fig. 2 Concentration and The Removal of Organic Matter in Relation to Time.

Table 2 Rate Constant Values for the Adsorption of Organics on ABAC.

Adsorption kinetic model	Model rate constant	Rate constant value	q_e, mg/g	R^2, -	RMSE, mg/g.min.
PFO	k_1, 1/min	0.048465	87.82	0.7108	6.55
PSO	k_2, g/mg min	0.000686	99.43	0.8998	3.86

The adsorption kinetics of organic matter on ABAC conformed predominantly to a PSO model, exhibiting a high R^2 value (0.8998) with relatively lower RMSE compared to PFO, as summarized in Table 2. In an environmental context, the PSO kinetic model effectively characterized the adsorption data of organic matter from aqueous solutions [48].

3.3.Mathematical Model Development

The dynamic behavior of the fixed-bed adsorption column was described using the advection–dispersion–adsorption model (ADAM). The ADAM is derived by applying a differential mass balance over a representative volume element of the packed bed. The accumulation of solute in the liquid phase is balanced by axial dispersion, convective transport, and adsorption onto the solid phase. The accumulation term can be written as Eq. (10).

$$Accumulation = \varepsilon_b \frac{\partial C}{\partial t} \quad \textbf{(10)}$$

The convective flux is described using Fick's law combined with advective transport as Eq. (11).

$$Flux = -D_{ax} \frac{\partial C}{\partial z} + v\, C \quad \textbf{(11)}$$

Combining these terms with the solid-phase accumulation yields the governing transient mass balance for the solute in the packed bed presented in Eq. (12). The model considers axial dispersion, convective transport in the fluid phase, and adsorption kinetics within the solid phase. The liquid-phase concentration is denoted by $C(z,t)$ (mg/L) while the solid-phase loading is denoted by $q(z,t)$ (mg/g). The axial coordinate and time are represented by z (m) and t (min), respectively.

$$\varepsilon_b \frac{\partial C}{\partial t} = D_{ax} \frac{\partial^2 C}{\partial z^2} - v \frac{\partial C}{\partial z} - (1-\varepsilon_b)\, \rho_p \frac{\partial q}{\partial t} \quad \textbf{(12)}$$

where ε_b is the bed porosity (0.4), D_{ax} is the axial dispersion coefficient (m^2/min), v is the interfacial velocity (m/min), and ρ_p is the apparent particle density (1188 g/L). The last term represents the rate of mass transfer from the fluid phase to the solid phase.

The equilibrium relationship between the liquid-phase concentration and the adsorbed phase was represented using the SAIM Eq. (7). The adsorption rate was described using the PSO kinetic model (Eq. (9)).

The adsorption column was initially assumed to be free of solute, $C(z,0)=0$, and $q(z,0)=0$. Constant concentration was imposed at the column inlet $C(0,t)=C_o$ (156 mg/L), while a zero-gradient condition was applied at the outlet $\left(\frac{\partial C}{\partial z}=0\right)_{z=L}$.

The dynamic performance of the adsorption column was evaluated using the breakthrough curve defined as C_{out}/C_{in}. The breakthrough time (t_b), saturation time (t_s), and total time (t_t) corresponding to selected ratios (5, 10, 50, and 90%) were determined. The mass transfer zone

(MTZ) was determined using Eq. (13), the dynamic adsorption capacity (q_{dyn}) of the column was calculated as Eq. (14), and the column efficiency η (%) was calculated by Eq. (15).

$$MTZ = L\left(1 - \frac{t_b}{t_s}\right) \quad \textbf{(13)}$$

$$q_{dyn} = \left(\frac{Q}{m_s}\right)\int \left(C_{in} - C_{out}\right) dt \quad \textbf{(14)}$$

$$\eta,\% = \left(1 - \frac{MTZ}{L}\right) \times 100 \quad \textbf{(15)}$$

Where Q is the volumetric flow rate (L/min), m_s is the adsorbent mass (g), and L is the adsorbent length (m).

The convective term was approximated using an upwind finite-difference scheme, while the axial dispersion term was evaluated using a second order central difference approximation. The resulting stiff ordinary differential equation system was integrated in time using the "solve_ivp" solver in Python (SciPy) with an implicit algorithm suitable for stiff problems. The inlet concentration was imposed as a Dirichlet boundary condition, while a zero-gradient condition was applied at the column outlet. The numerical solution provided the breakthrough curves along the adsorption time, as shown in Figs. 3 to 5, for the design parameters studied, which were: liquid interfacial velocity, adsorber bed height, and inlet organic pollutants concentration.

3.4.1.Effect of Liquid Interfacial Velocity (v)

The effect of liquid interfacial velocity on the dynamic performance of the adsorption column was investigated via simulation, and the results were illustrated in Fig. 3. Table 3 summarizes the important design values. The breakthrough time decreased, and the slope of the adsorption front increased with increasing fluid velocity from 0.0125 to 0.0313 m/min, as shown in Fig. 3. Explicitly, the adsorption layer remained effective for a much longer period before breakthrough began at the lowest velocity, while at the highest interfacial velocity, the column approached saturation much earlier. This behavior is physically expected, as increasing the linear interfacial velocity of the fluid through the packed adsorption column reduces the residence time within the adsorption bed, decreases the contact time between the contaminating fluid and the ABAC (adsorbent), and simultaneously limits the time available for outward mass transfer and particle adsorption. Under these conditions, a faster propagation of the adsorption front is observed, and the adsorption bed reaches saturation sooner. The same trend was reported in a previous study of the adsorption of ciprofloxacin, bisphenol A, oily wastewater, and lead (II), where those studies indicated that a higher flow rate accelerates breakthrough and depletion because the solute has less time to diffuse into the porous structure of the adsorbent [49, 50]. The numerical results (Table 3) also show a gradual increase in the length of the mass-transfer zone with increasing velocity. As the interfacial velocity increased, the calculated MTZ value increased from 0.292 to 0.556 m, indicating a stretching of the mass transfer front relative to the length of the adsorption bed at higher velocity. This is scientifically logical, as a short contact time already reduces the solute's ability to achieve local equilibrium with the heterogeneous adsorption sites described by the SAIM, while the kinetic formula of PSO still imposes a limited adsorption resistance. Consequently, the adsorption zone expands and moves more rapidly through the adsorption column. The results also showed a slight increase in the dynamic adsorption capacity, q_{dyn}, from 4.45 to 5.09 mg/g, indicating an improvement in the adsorption bed utilization per unit mass before reaching saturation with a moderate increase in fluid flow velocity. However, the operating time becomes significantly shorter, and the column efficiency decreased from 70.8% at the lowest velocity to 44.4% at the highest interfacial velocity.

3.4.2.Effect of Adsorber Bed Height (L)

The simulated results of the effect of adsorber bed height on breakthrough characteristics were plotted in Fig. 4, and the numerical results were summarized in Table 4. Increasing the adsorber bed height from 0.60 to 1.00 m resulted in a clear shift in the breakthrough curves towards a longer operating time range, with a noticeable delay in both breakthrough and approach to depletion. This classic response indicated that as increasing the bed height leads to an increase in the amount of adsorbent and consequently an increase in the number of active adsorption sites. Furthermore, higher bed heights provide a longer transport distance for the adsorption front and increase the effective contact time between the pollutant and the adsorbent phase. This behavior is highly consistent with the behavior reported previously [49,51], where increasing the adsorbent bed height resulted in delayed breakthrough curves and thus the ability to treat larger volumes of contaminated wastewater before depletion. The absolute MTZ length increased slightly with the height of the adsorption bed, the MTZ/L ratio decreased (Table 4), causing an increase in the adsorption column, allowing for the efficient use of a larger portion of the adsorbent before breakthrough occurred. Moreover, a delay in breakthrough and saturation times was observed when the height of the adsorbent bed increased from

0.60 to 1.00 m, as shown in Fig. 4 and Table 4. The estimated MTZ increased from 0.36 to 0.45 m² with increasing adsorption ABAC bed height, thus providing more active adsorption sites and a longer axial distance for progressive adsorption, which improved the efficiency of the adsorption column. Conversely, the calculated q_{dyn} value decreased slightly from 5.67 to 4.97 mg/g with increasing adsorption bed height. The higher adsorption bed performance does not necessarily mean it was worse; this is a common outcome in fixed-bed adsorption systems, especially when a portion of the deeper bed remains unused until later stages of operation [52].

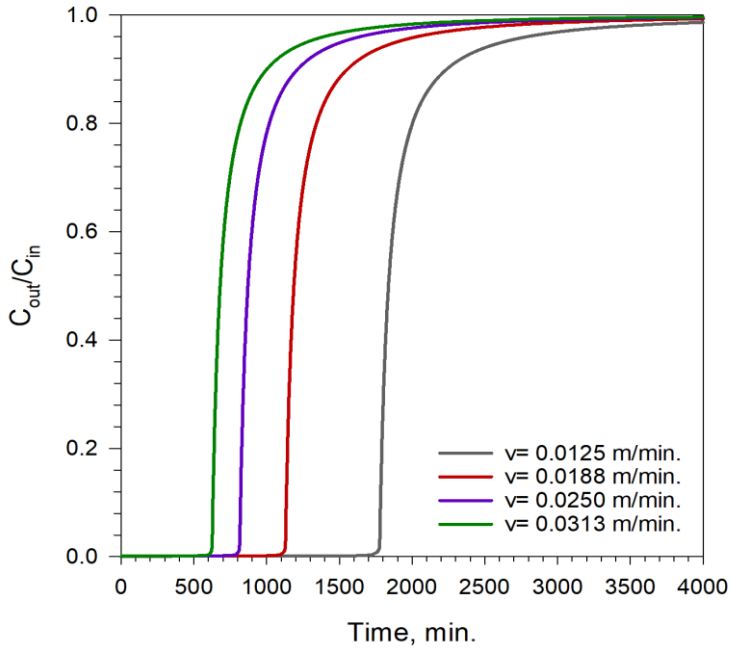


Fig. 3 Simulated Breakthrough Curves Using ADAM Under Different Liquid Interfacial Velocity for 1 m Adsorber Bed Length And 156 mg/L Inlet Concentration.

Table 3 Effect of Liquid Interfacial Velocity for 1 m Adsorber Bed Height And 156 mg/L Inlet Concentration.

v, m/min	t_b, min	t_s, min	t_t, min	MTZ, m	MTZ/L, -	q_{dyn}, mg/g	η, %
0.0125	1770	2500	2135	0.292	0.292	4.45	70.8
0.0188	1120	1800	1460	0.378	0.378	4.57	62.2
0.0250	810	1550	1180	0.477	0.477	4.92	52.3
0.0313	600	1350	975	0.556	0.556	5.09	44.4

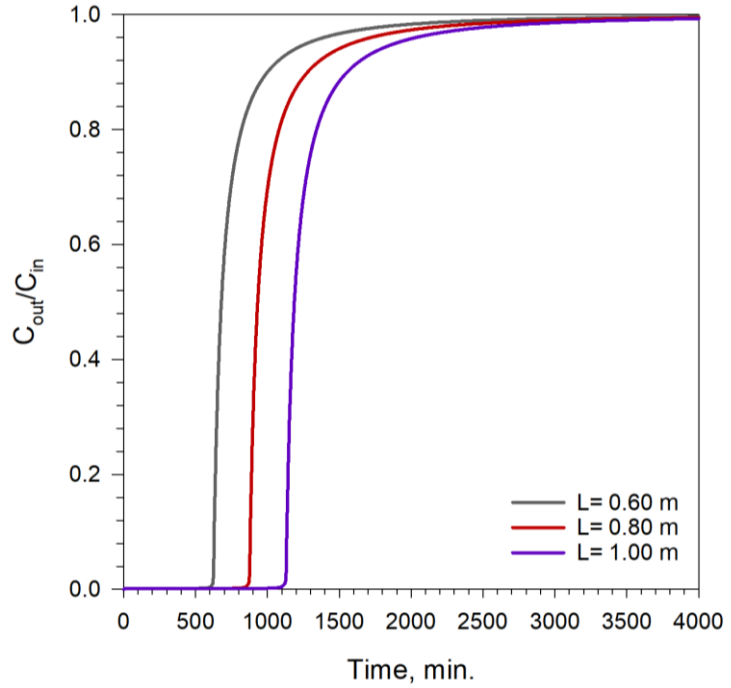


Fig. 4 Simulated Breakthrough Curves Using ADAM Under Different Adsorber Bed Heights For 0.0188 m/min. Liquid Interfacial Velocity and 156 mg/L Inlet Concentration.

Table 4 Effect of Adsorber Bed Height for 0.0188 m/min Liquid Interfacial Velocity and 156 mg/L Inlet Concentration.

L, m	t_b, min	t_s, min	t_t, min	MTZ, m	MTZ/L, -	q_{dyn}, mg/g	η, %
0.60	620	1550	1085	0.360	0.60	5.67	40.0
0.80	870	1800	1335	0.413	0.52	5.23	48.4
1.00	1120	2050	1585	0.454	0.45	4.97	54.6

3.4.3.Effect of Inlet Concentration (Co)

Column simulated breakthrough curves were found to vary with influent organic matter concentration (as COD), as depicted in Fig. 5, and the essential numerical design values were tabulated in Table 5. The results clearly indicated a shift in the breakthrough, resulting in a marked decrease in breakthrough time, as the inlet concentration of organic pollutants in the wastewater increased from 100 to 400 mg/L. Higher inlet adsorbate concentrations cause faster saturation of the adsorption bed due to an increase in the mass transfer driving force (concentration difference) between the liquid and the adsorbent surface, which enhances the apparent mass transfer rate and leads to faster occupancy of the active adsorption sites available near the inlet of the adsorption bed. Although increasing the concentration difference correspondingly accelerates adsorption bed saturation and reduces the effective operating time of the column. This is consistent with previous work [53], where using an inlet with a high adsorbate concentration resulted in steeper curves and shorter breakthrough and depletion times due to faster saturation of active sites and a narrower apparent breakthrough region. Numerically (as shown in Table 5), increasing the feed concentration from 100 to 400 mg/L reduced the approximate breakthrough time from about 1770 min to 390 min, with a simultaneous reduction in the near-exhaustion time from about 2500 min to 1100 min. The observed acceleration in saturation again arises from concentration effects and not from hydrodynamic changes in the constant Reynolds number. The driving force of localized mass transfer increases due to the greater concentration gradient at the bed inlet, and it rapidly occupies available sites, explaining the steeper fronts clearly observed in Fig. 5.

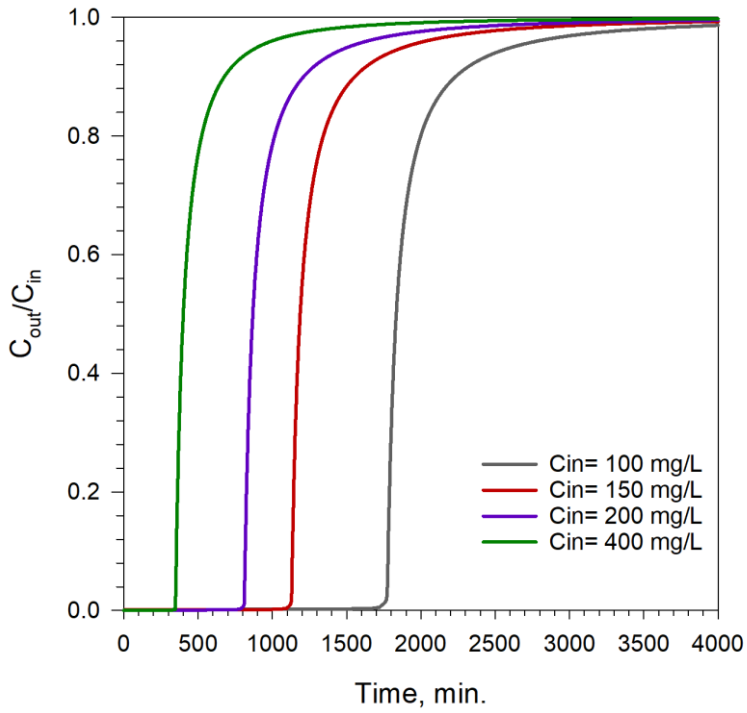


Fig. 5 Simulated Breakthrough Curves Using ADAM Under Different Inlet Concentrations For 1 m Adsorber Bed Height and 0.0188 M/Min Liquid Interfacial Velocity.

Table 5 Effect of Inlet Concentration for 1 m Adsorber Bed Height and 0.0188 m/min Liquid Interfacial Velocity.

C_{in}, mg/L	t_b, min	t_s, min	t_t, min	MTZ, m	MTZ/L, -	q_{dyn}, mg/g	η, %
100	1770	2500	2135	0.292	0.292	4.46	70.8
150	1120	1800	1460	0.378	0.378	4.57	62.2
200	810	1550	1180	0.477	0.477	4.93	52.3
400	360	1100	730	0.673	0.673	6.10	32.7

3.4.4.Design Implications and Bed Utilization

Figures 3, 4, and 5 confirm the expected dynamic design logic for fixed-bed operation: lower velocity, greater bed height, and lower influent concentration favor longer service time before breakthrough. This conclusion is in good agreement with the reference ciprofloxacin study (30). Nevertheless, the present curves appear more strongly fronted, which is plausibly related to the use of the SAIM/PSO framework rather than the LAIM/PFO combination adopted in the attached work. The sharper fronts in the present simulation suggest a stronger sensitivity of uptake rate to local concentration and remaining site availability, which may be advantageous for parametric design but should ultimately be validated against experimental breakthrough data before final scale-up. From a process design perspective, column efficiency is closely related to bed utilization efficiency. High efficiency values indicate that most of the adsorbents in the column actively participate in the adsorption process before breakthrough occurs. Conversely, low efficiency values indicate that a significant portion of the ABAC bed remains unused at the time of breakthrough. The results obtained in this study clearly demonstrate that operating conditions that minimize the relative size of the MTZ lead to improved bed utilization. Lower velocities and larger bed heights are therefore desirable for maximizing column efficiency and extending operational lifetime.

4.CONCLUSIONS

ABAC demonstrated remarkable efficiency and promise as an adsorbent for real-world municipal wastewater treatment. Batch adsorption experiments showed that the SAIM model accurately described equilibrium behavior, reflecting the heterogeneous surface nature and the multiple adsorption mechanisms associated with organic matter as measured by COD. The maximum adsorption capacity reached 156.38 mg/g, a direct indicator of ABAC's ability to remove a complex mixture of organic pollutants. In terms of kinetics, PSO model proved to be the most consistent with the data, indicating that the process rate is governed more by the availability of active sites than solely by diffusion mechanisms. A mathematical model based on experimental parameters was developed to simulate the behavior of a fixed-bed adsorption column. The simulation successfully reproduced the breakthrough curves under various operational variables, such as flow velocity, bed height, and incoming pollutant concentration. These results allowed for the estimation of key design parameters such as t_b, MTZ, q_{dyn}, and column efficiency, which reached 70.8% under optimal operating conditions, reflecting the promising efficiency of ABAC material in the adsorption of organic pollutants on an industrial scale.

NOMENCLATURE

b	LAIM constant or the energy or net enthalpy of adsorption, L/mg
b_T	Temkin isotherm constant
C_e	Equilibrium concentration of adsorbate in the liquid phase, mg/L
C_o	Initial concentration of ABAC in the fluid phase, mg/L
k_1	PFO adsorption rate constant, 1/min
k_2	PSO adsorption rate constant, g/mg.min
K_{ad}	D–R isotherm constant adsorption, mol²/kJ²
K_F	Freundlich constant indicative of the relative adsorption capacity, mg/g
K_s	Sips model constant, L/mg
k_T	Equilibrium binding constant of the Temkin isotherm
L	Adsorbent length, m
m	Mass of the adsorbent, g
n_s	Exponent of the SAIM
q_e	Equilibrium concentration of adsorbate in the adsorbent phase, mg/g
q_{max}	Maximum monolayer coverage capacity, mg/g
q_s	theoretical saturation capacity, mg/g
Q	Volumetric flow rate, L/min
t	time, min
T	Temperature, K
V	Volume of fluid phase, L
Greek symbols	
ε_b	Bed porosity
v	Interfacial velocity, m/min
ρ_p	Apparent particle density, g/L
Subscripts	
b	breakthrough curves
s	Simultaneous reduction in the near-exhaustion
t	Total exhaustion

REFERENCES

[1] Omer AM, Abd El-Monaem EM, Eltaweil AS. **Novel Reusable Amine-Functionalized Cellulose Acetate Beads Impregnated Aminated Graphene Oxide for Adsorptive Removal of Hexavalent Chromium Ions**. *International Journal of Biological Macromolecules* 2022; **208**: 925–34.

[2] Abd El-Monaem EM, Eltaweil AS, Elshishini HM, Hosny M, Abou Alsoaud MM, Attia NF, et al. **Sustainable Adsorptive Removal of Antibiotic Residues by Chitosan Composites: An Insight into Current Developments and Future Recommendations**. *Arabian Journal of Chemistry* 2022; **15**(5): 103743.

[3] Anyanwu IN, Beggel S, Sikoki FD, Okuku EO, Unyimadu JP, Geist J. **Pollution of the Niger Delta with Total Petroleum Hydrocarbons, Heavy Metals and Nutrients in Relation to Seasonal Dynamics**. *Scientific Reports* 2023; **13**(1).

[4] Rafiq A, Ikram M, Ali S, Niaz F, Khan M, Khan Q, et al. **Photocatalytic Degradation of Dyes Using Semiconductor Photocatalysts to Clean Industrial Water Pollution**. *Journal of Industrial and Engineering Chemistry* 2021; **97**: 111–28.

[5] Patel M, Kumar R, Kishor K, Mlsna T, Pittman CUJ, Mohan D. **Pharmaceuticals of Emerging Concern in Aquatic Systems:**

Chemistry, Occurrence, Effects, and Removal Methods. *Chemical Reviews* 2019; **119**(6): 3510–673.

[6] Gkika DA, Tolkou AK, Evgenidou E, Bikiaris DN, Lambropoulou DA, Mitropoulos AC, et al. **Fate and Removal of Microplastics from Industrial Wastewaters**. *Sustainability* 2023; **15**(8): 6969.

[7] Wagner M, Lambert S. **Freshwater Microplastics - The Handbook of Environmental Chemistry**. Springer Nature 2018: 58.

[8] Tchobanoglous G, Burton FL, Stensel HD, others. **Wastewater Engineering: Treatment and Reuse**. McGraw-Hill, Inc: New York; 2003.

[9] Owen M. **Ensure Availability and Sustainable Management of Water and Sanitation for All**. Oxford University Press eBooks 2023.

[10] Organization WH. **Guidelines for the Safe Use of Wastewater, Excreta and Greywater**. World Health Organization 2006.

[11] Al-Kindi GY, Al-Sultan AA. **Evaluation of Environmental Quality for Al-Razzaza Lake in Iraq**. *Innovative Infrastructure Solutions* 2024; **9**(11): 418.

[12] Shah AI, Din Dar MU, Bhat RA, Singh JP, Singh K, Bhat SA. **Prospectives and Challenges of Wastewater Treatment Technologies to Combat Contaminants of Emerging Concerns**. *Ecological Engineering* 2020; **152**: 105882.

[13] Khanzada NK, Farid MU, Kharraz JA, Choi J, Tang CY, Nghiem LD, et al. **Removal of Organic Micropollutants Using Advanced Membrane-Based Water and Wastewater Treatment: A Review**. *Journal of Membrane Science* 2020; **598**: 117672.

[14] Gupta AK, Uddameri V, Majumder A, Nimbhorkar SK. **Wastewater Engineering: Issues, Trends, and Solutions**. Taylor & Francis eBooks 2023.

[15] Saravanan A, Senthil Kumar P, Rangasamy G, Hariharan R, Hemavathy R V., Deepika PD, et al. **Strategies for Enhancing the Efficacy of Anaerobic Digestion of Food Industry Wastewater: An Insight into Bioreactor Types, Challenges, and Future Scope**. *Chemosphere* 2023; **310**.

[16] Kamal SK, Mohammed AE, Alabdraba WM, Hamed HH, Waly KA. **Industrial Wastewater Treatment in North Gas Company by Using Coagulation – Flocculation Process**. *Journal of Petroleum Research and Studies* 2020; **10**(4): 252–69.

[17] Judd S. **The MBR Book: Principles and Applications of Membrane Bioreactors in Water and Wastewater Treatment**. Elsevier 2006.

[18] Ahmed MB, Zhou JL, Ngo HH, Guo W. **Adsorptive Removal of Antibiotics from Water and Wastewater: Progress and Challenges**. *Science of The Total Environment* 2015; **532**: 112–26.

[19] Abbas AS, Darweesh TM. **Preparation and Characterization of Activated Carbon for Adsorption of Fluoroquinolones Antibiotics**. *Journal of Engineering* 2016; **22**(8): 140–57.

[20] Barno SKA, Mohamed HJ, Saeed SM, Al-Ani MJ, Abbas AS. **Prepared 13X Zeolite as a Promising Adsorbent for the Removal of Brilliant Blue Dye from Wastewater**. *Iraqi Journal of Chemical and Petroleum Engineering* 2021; **22**(2).

[21] Wang S, Peng Y. **Natural Zeolites as Effective Adsorbents in Water and Wastewater Treatment**. *Chemical Engineering Journal* 2010; **156**(1): 11–24.

[22] Li Y, Liu Y, Tang H, Dong S. **Oxidized Cross-Linked Guar Gum with Hydrophobic Groups: Structure, Properties and Removal of Reactive Blue-XBR in Simulated Water**. *Arabian Journal for Science and Engineering* 2018; **43**(7): 3621–9.

[23] Zhou Y, Zhang M, Wang X, Huang Q, Min Y, Ma T, et al. **Removal of Crystal Violet by a Novel Cellulose-Based Adsorbent: Comparison with Native Cellulose**. *Industrial & Engineering Chemistry Research* 2014; **53**(13): 5498–506.

[24] Kyzas G, Bikiaris D. **Recent Modifications of Chitosan for Adsorption Applications: A Critical and Systematic Review**. *Marine Drugs* 2015; **13**(1): 312–37.

[25] Mall ID, Srivastava VC, Agarwal NK. **Removal of Orange-G and Methyl Violet Dyes by Adsorption onto Bagasse Fly Ash—Kinetic Study and Equilibrium Isotherm Analyses**. *Dyes and Pigments* 2006; **69**(3): 210–23.

[26] Hameed BH, El-Khaiary MI. **Equilibrium, Kinetics and Mechanism of Malachite Green Adsorption on Activated Carbon Prepared from Bamboo by K2CO3 Activation and Subsequent Gasification with CO2**. *Journal of Hazardous Materials* 2008; **157**(2–3): 344–51.

[27] Abbas H, Abbas AS. **Adsorption of Flagyl on Prepared Ash from Rice**

Husk. *Iraqi Journal of Chemical and Petroleum Engineering* 2021; **22**(4): 11–7.

[28] Bhatnagar A, Sillanpää M. **Utilization of Agro-Industrial and Municipal Waste Materials as Potential Adsorbents for Water Treatment—A Review**. *Chemical Engineering Journal* 2010; **157**(2–3): 277–96.

[29] Ahmed MJ, Theydan SK. **Fluoroquinolones Antibiotics Adsorption onto Microporous Activated Carbon from Lignocellulosic Biomass by Microwave Pyrolysis**. *Journal of the Taiwan Institute of Chemical Engineers* 2014; **45**(1): 219–26.

[30] Al-Jubory FK, Abbas AS, Mujtaba IM. **Adsorptive Removal of Ciprofloxacin from Simulated Wastewater Using Crosslinked Starch Ester: Isotherms, Kinetics, Thermodynamics, Modeling, and Simulation for Continuous Operation**. *Chemical Engineering Research and Design* 2023; **200**: 332–43.

[31] Barno SKA, Abbas AS. **Reduction of Organics in Dairy Wastewater by Adsorption on a Prepared Charcoal from Iraqi Sugarcane**. *IOP Conference Series: Materials Science and Engineering* 2020; **736**(2): 022096.

[32] Faisal HA, Mohammed AK, Al Sbani NH, Isaha WNRW. **Comparative Study of Activated Carbon and Silver Nanoparticle-Loaded Activated Carbon Derived from Tea Waste for Removal of Tetracycline from Aqueous Solution**. *Tikrit Journal of Engineering Sciences* 2025; **32**(2): 1890.

[33] Wang L, Ma L, Wang J, Zhao X, Jing Y, Liu C, et al. **Research Progress on the Removal of Contaminants from Wastewater by Constructed Wetland Substrate: A Review**. *Water (Basel)* 2024; **16**(13): 1848.

[34] Poudel A. **Anthracite as Filter Media in Filtration Process**. *Journal of Advanced College of Engineering and Management* 2021; **6**: 1–7.

[35] Salman RH, Khudhair EM, Abed KM, Abbas AS. **Removal of E133 Brilliant Blue Dye from Artificial Wastewater by Electrocoagulation Using Cans Waste as Electrodes**. *Environmental Progress & Sustainable Energy* 2024; **43**(2).

[36] Chowdhury ZZ, Hamid SBA, Zain SM. **Evaluating Design Parameters for Breakthrough Curve Analysis and Kinetics of Fixed Bed Columns for Cu(II) Cations Using Lignocellulosic Wastes**. *Bioresources* 2014; **10**(1).

[37] Abdulrahman MS, Alsarayreh AA, Barno SKA, Abd Elkawi MA, Abbas AS. **Activated Carbon from Sugarcane as an Efficient Adsorbent for Phenol from Petroleum Refinery Wastewater: Equilibrium, Kinetic, and Thermodynamic Study**. *Open Engineering* 2023; **13**(1).

[38] Foo KY, Hameed BH. **Insights Into the Modeling of Adsorption Isotherm Systems**. *Chemical Engineering Journal* 2010; **156**(1): 2–10.

[39] Srivastava VC, Swamy MM, Mall ID, Prasad B, Mishra IM. **Adsorptive Removal of Phenol by Bagasse Fly Ash and Activated Carbon: Equilibrium, Kinetics and Thermodynamics**. *Colloids and Surfaces A: Physicochemical and Engineering Aspects* 2006; **272**(1–2): 89–104.

[40] Yan LG, Qin LL, Yu HQ, Li S, Shan RR, Du B. **Adsorption of Acid Dyes from Aqueous Solution by CTMAB Modified Bentonite: Kinetic and Isotherm Modeling**. *Journal of Molecular Liquids* 2015; **211**: 1074–81.

[41] Langmuir I. **The Constitution and Fundamental Properties of Solids and Liquids. Part I. Solids**. *Journal of the American Chemical Society* 1916; **38**(11): 2221–95.

[42] Freundlich H. **Über Die Adsorption in Lösungen**. *Zeitschrift für Physikalische Chemie* 1906; **57**U(1): 385–470.

[43] Temkin M, Pyzhev V. **Kinetics of the Synthesis of Ammonia on Promoted Iron Catalysts**. *Acta Physicochimica URSS* 1940; **12**(1): 327–56.

[44] Grishchenko L, Diyuk V, Konoplitska O, Lisnyak V, Maryichuk R. **Modeling of Copper Ions Adsorption onto Oxidative-Modified Activated Carbons**. *Adsorption Science & Technology* 2017; **35**(9–10): 884–900.

[45] Jin GP, Zhu XH, Li CY, Fu Y, Guan JX, Wu XP. **Tetraoxalyl Ethylenediamine Melamine Resin Functionalized Coconut Active Charcoal for Adsorptive Removal of Ni(II), Pb(II) and Cd(II) From Their Aqueous Solution**. *Journal of Environmental Chemical Engineering* 2013; **1**(4): 736–45.

[46] Lagergren S. **About the Theory of So-Called Adsorption of Soluble Substances**. *Kungliga Svenska Vetenskapsakademiens Handlingar* 1898; **24**: 1–39.

[47] Ho YS, McKay G. **Pseudo-Second Order Model for Sorption Processes**. *Process Biochemistry* 1999; **34**(5): 451–65.

[48] Mojoudi N, Mirghaffari N, Soleimani M, Shariatmadari H, Belver C, Bedia J. **Phenol Adsorption on High Microporous Activated Carbons Prepared from Oily Sludge: Equilibrium, Kinetic and Thermodynamic Studies**. *Scientific Reports* 2019; **9**(1).

[49] Matharage H, Jayaweera M, Bandara N, Manatunge J, Jayawardana D, Dissanayake J. **Fixed-Bed Column Studies on the Adsorption of Bisphenol A From Aqueous Solutions Using Chemically Activated King Coconut Biochar**. *Discover Chemical Engineering* 2025; **5**(1).

[50] Sarran MA, AbdulRazak AA, Abid MF, Jawad Al-Bayati AD, Rashid KT, Shehab MA, et al. **Oily Wastewater Treatment by Using Fe3O4/Bentonite in Fixed-Bed Adsorption Column**. *Chemical Engineering* 2024; **8**(5).

[51] Zhu H, Huang Q, Shi M, Fu S, Zhang X, Yang Z, et al. **Adsorption of Sb(III) From Aqueous Solution by nZVI/AC: A Magnetic Fixed-Bed Column Study**. *Nanomaterials* 2021; **11**(8).

[52] Patel H. **Fixed-Bed Column Adsorption Study: A Comprehensive Review**. *Applied Water Science* 2019; **9**(3): 45.

[53] Thomas WJ, Crittenden BD. **Adsorption Technology and Design**. Butterworth-Heinemann 1998.